Apparent Rate Constant Mapping Using Hyperpolarized [1-^{13}C]Pyruvate

Oleksandr Khegai[1,2], Rolf F Schulte[2], Martin A Janich[2], Marion I Menzel[2], Eliane Farrell[3], Angela M Otto[4], Jan Henrik Ardenkjaer-Larsen[5,6], Steffen J Glaser[1], Axel Haase[4], Markus Schwaiger[3], and Florian Wiesinger[2]

[1]*Department of Chemistry, Technische Universität München, Munich, Germany,* [2]*GE Global Research, Munich, Germany,* [3]*Institute of Nuclear Medicine, Technische Universität München, Munich, Germany,* [4]*Institute of Medical Engineering, Technische Universität München, Munich, Germany,* [5]*MST-ASL MR, GE Healthcare, Copenhagen, Denmark,* [6]*Department of Electrical Engineering, Technical University of Denmark, Copenhagen, Denmark*

Introduction:

Dissolution dynamic nuclear polarization (DNP) enables MR signal enhancement of [1-^{13}C]pyruvate in liquid state by up to five orders of magnitude compared to thermal equilibrium (1). High sensitivity of this technique allows in vivo measurement of metabolic fluxes in real time using magnetic resonance spectroscopy (2). Biologically, after injection and perfusion, pyruvate is absorbed by tissues and enzymatically metabolized into downstream metabolites such as lactate, alanine, and bicarbonate. Quantitative kinetic information of pyruvate metabolism in tissue is of great interest as a key characteristic of some diseases. Therefore, the aim of this work is to develop comprehensive methods for the quantification, interpretation and visualization of dynamic hyperpolarized ^{13}C metabolite signals.

Methods:

Temporally resolved spectral-spatial data were acquired using IDEAL spiral chemical shift imaging (CSI) (3). Applying a two-site exchange kinetic model (4), the temporal dimension is compressed into two characteristic rate constants: i) the apparent build-up rate of downstream metabolites from pyruvate $k_{pyr\to m}$, and ii) an effective decay rate $R_{eff,m}$ describing the cumulative effect of repetitive excitation, T_1-relaxation and backward conversion. In a time-discretized formulation this leads to following rate equation:

$$da_m(t)/dt = +k_{pyr\to m}a_{pyr}(t) - R_{eff,m}a_m(t) \quad [1]$$

with a_{pyr} and a_m denoting signals of the pyruvate substrate and a certain downstream metabolite m, respectively. Transforming Eq. [1] from time to frequency domain results into:

$$i\Omega\tilde{a}_m(\Omega) = +k_{pyr\to m}\tilde{a}_{pyr}(\Omega) - R_{eff,m}\tilde{a}_m(\Omega) \quad [2]$$

with $\tilde{a}_{pyr}(\Omega)$ and $\tilde{a}_m(\Omega)$ Fourier transform of $a_{pyr}(t)$ and $a_m(t)$. Both in time and frequency domain, Eq. [1] and [2] lead to over-determined systems of linear equations, which can be solved for $k_{pyr\to m}$ and $R_{eff,m}$ using the Moore-Penrose pseudo-inverse. Interestingly for Ω=0, Eq. [2] provides a clear physical interpretation of the often used ratio of time-integrated metabolite signals

$$\int a_m(t)\,dt / \int a_{pyr}(t)dt = \tilde{a}_m(0)/\tilde{a}_{pyr}(0) = k_{pyr\to m}/R_{eff,m} \quad [3].$$

Conceptually, the proposed kinetic model accounts for variable inflow and outflow of pyruvate but assumes them to be the same (or negligible) for the downstream metabolite m. This formulation decouples the kinetics between pyruvate and its metabolic products into single differential equations. As a consequence, in this description no explicit arterial input function is required, as it is implicitly contained in the pyruvate signals.

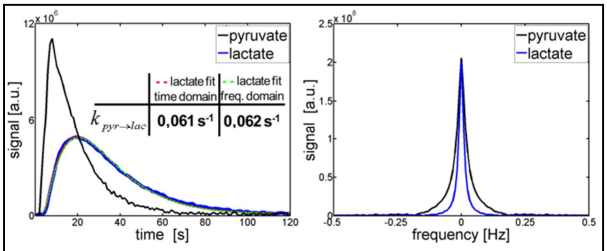

Figure 1. Typical in vivo metabolite signals in tumor area in time (left) and frequency (right) domains. The similar signal intensity of pyruvate and lactate at Ω =0 in frequency domain can be explained by the estimated ratio $k_{pyr\to lac}/R_{eff,lac} = \tilde{a}_{lac}(0)/\tilde{a}_{pyr}(0) \approx 1$

Experiments:

[1-^{13}C]pyruvate was polarized using a HyperSense DNP polarizer and subsequently dissolved to a concentration of 80 mM. A volume of 2.5 mL/kg (body mass) was injected into the tail vein of four adult female Fischer rats bearing subcutaneous mammary adenocarcinomas. The measurements were performed on a 3T GE Signa HDx MRI scanner with a dual-tuned ^{1}H/^{13}C volume coil using IDEAL spiral CSI, consisting of 7 echo time shifted (ΔTE = 1.12 ms) singe-shot spirals (α= 10°, TR= 500 ms, FOV=80 mm, nominal matrix resolution 32x32, 62.5 kHz acquisition bandwidth, 45 ms readout) plus one additional FID acquisition. This allowed dynamic, multi-slice (4 slices, 10 mm thickness) CS imaging with a temporal resolution of 4 s.

Results and Discussion:

Typical metabolite signals in time and frequency domain are illustrated in Fig. 1, demonstrating a sparse, DC-centered signal representation in the frequency domain. The main advantage of the frequency description is a natural compression of the signal dynamics into a few dominant Fourier coefficients and the avoidance of time differentiation, which generally results in noise amplification.

Figure 2 displays tumor slices in four rats in the form of time-integrated metabolite images of pyruvate (a) and lactate (b), ratios of time-integrated signals of lactate and pyruvate normalized by an average decay rate $\bar{R}_{eff,lac}$= 0.1 s^{-1} (c) and apparent build-up rate constant maps of lactate estimated in time (d) and frequency (e) domain. The data are displayed in form of image overlays using a high resolution gradient echo image of identical scan geometry as anatomical reference. The apparent build-up rate constant maps comprehensively visualize metabolic activity of underlying tissues and organs in a quantitative and spatially resolved manner. Eq. [3] shows the linear relationship between the apparent build-up rate constant and the ratio of time-integrated metabolite signals with the apparent decay rate $R_{eff,m}$ as a proportional coefficient. The later can be estimated from signal depletion due to repetitive excitation and assuming a constant T_1 relaxation time for lactate and negligible backward conversion as $\bar{R}_{eff,lac} \approx 0.1\ s^{-1}$. The improved contrast provided by the apparent build-up rate maps (d,e) clearly identifies the tumor location as regions of enhanced metabolism with $k_{pyr\to lac} \approx 0.1$ s^{-1}. Similar contrast behavior was obtained from the ratio of time-integrated metabolite signals normalized by the averaged decay rate (c). This method is more advantageous for data with low SNR, but quantitatively somewhat less accurate, due to the underlying assumption of an equal apparent decay rate in all pixels. The utility of the apparent build-up rate constant mapping for the localization and characterization of tumors and their response to therapy needs to be further investigated in dedicated studies.

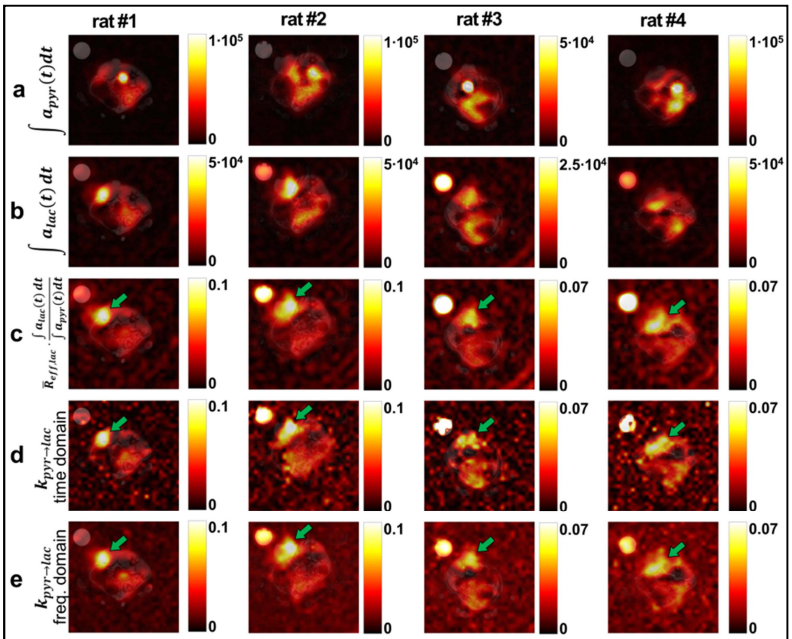

Figure 2. Time-integrated metabolite maps of pyruvate and lactate (a,b, in a.u.), normalized by $\bar{R}_{eff,lac}$= 0.1 s^{-1} ratio of time-integrated metabolite signals (c, in s^{-1}), and time (d, in s^{-1}) and frequency (e, in s^{-1}) domain derived apparent build-up rate constant maps of lactate in tumor slices of 4 different animals. A syringe containing [1-^{13}C]lactate (at the top-left corner of each image) was used as a reference for both ^{13}C and proton images. High apparent build-up rate constants in the tumor (green arrows) indicate its high metabolic activity.

References: (1) JH Ardenkjaer-Larsen et. al., PNAS 100:10158(2003) (2) K Golman et al, PNAS, 100:10435(2003) (3) F Wiesinger et. al. MRM 68(1):8-16(2012) (4) SE Day et. al., Nat Med 13(11):1382-1387(2007)

Acknowledgements: Co-funding by BMBF grants #01EZ0826/7, #01EZ1114 and the TUM Graduate School of Information Science in Health.